ARCHIVES OF ELECTRICAL ENGINEERING VOL. 67(4), pp. 773–788 (2018)

DOI 10.24425/aee.2018.124739

Direct predictive control of asynchronous machine torque using matrix converter

VAHID TALAVAT, SADJAD GALVANI, MAHDI HAJIBEIGY

Faculty of Electrical and Computer Engineering, Urmia University
Iran, Urmia city, 11km SERO Road, postal code:5756151818
e-mail: st_m.hajibeigy@urmia.ac.ir

(Received: 10.02.2018, revised: 19.07.2018)

Abstract: The matrix converter is a new generation of power electronic converters and is an alternative to back-to-back converters in applications that dimensions and weight are important. In this paper, a simple control algorithm for a three-phase asynchronous motor based on a direct torque control technique, which is fed through a three-phase direct matrix converter, is presented. For direct matrix converters, 27 switching modes are possible, which using the predictive control technique and for the different modes of the matrix converter, the motor behavior is estimated at the next sampling interval. Then the objective function is determined and the optimal possible mode is selected. Finally, the best switching mode is applied to the direct matrix converter. In order to evaluate the proposed method, simulation of the system in Matlab/Simulink software environment is performed. The results show the effectiveness of the proposed method.

Key words: asynchronous motor, direct predictive control of torque, direct matrix converter

1. Introduction

Due to the growth of industrialization and the expansion of the use of electric motors, attention to their control plans has increased to improve their capabilities. Today, about 90 percent of the world's electric motors are three-phase induction motors and improving the drive of these motors due to rising energy prices and the growth of power electronics devices, has been accelerated [1, 2].

The direct torque control method, as one of the control methods of the induction motors, provides the ability to achieve the proper torque control performance without the need for a speed sensor. On the other hand, the above method has disadvantages such as the complexity of controlling flux and torque at very low speeds, high ripples of current and torque, variable switching frequency, high turbulence at low speeds and the impossibility of direct control over the current.

In recent decades, extensive research has been done to improve the above problems [2]. Use of modified switching tables, modification of switching patterns, correction of comparators with

(without) two and three-level hysteresis limiter, applying fuzzy and neuro-fuzzy methods, using modified flux estimators to improve their performance at low speeds, and finally applying PWM and SVM-based methods for fixing the switching frequency.

The theory of predictive control, which was introduced in the late 1970s, has advantages that make it easy to use in drive applications. On the other hand, its idea is understandable and simple to apply to a variety of systems [1]. In [1], various predictive control methods in power electronics and drive of electric machines have been investigated. Also a simple classification for a variety of predictive control methods. In [2], a torque predictive control method based on the discrete state space model of machine which includes the term of time variant rotor speed, is presented. Using this method, the accuracy of the state estimation is significantly improved compared to the conventional Euler approximation. In [3], a predictive torque control method is proposed for variable speed performance of high performance multi-phase drives.

In recent years, due to advances in power electronics, the use of three-phase drives has increased. Meanwhile, the use of matrix converters has become more important because of its advantages [3]. The advantage of using matrix converters in electric drives is that, despite the smaller volume of the converter and the lack of a DC link capacitor, it is possible to bidirectionally transfer electrical power from an AC network to a motor and vice versa and at the same time, the input power factor is near the unit. On the other hand, harmonic injection to the AC network is also prevented. In [4], an integrated structure including a frequency converter and a motor based on the matrix converter is provided for industrial applications. This design uses bidirectional switches. In [5], a predictive scheme is presented to reduce the flux and torque ripples in the direct torque control method.

The proposed method is implemented on the basis of the direct control of the torque and compensates the delay which is due to the processing of information. In [6], the use of full-order and reduced order observers is proposed for predictive control without torque robust sensor in induction motors. The predictive torque control of the induction motor with a variable switching point is investigated in [7]. By using this method, along with adjusting the torque and flux in reference values, a new control objective function is also created to minimize the torque ripple.

An integrated control strategy based on the phase angle estimation for a matrix converter interface system has been studied in [8]. In [9], a systematic approach is proposed to achieve the dynamic model of a matrix converter.

The purpose of this model is to design a controller for a matrix converter that controls the active and reactive power flow from the power source to the network. In [10], an alternative method of space vector modulation for matrix converters is proposed that reduces the time of the common mode output voltage.

In this paper, a simple control algorithm for a three-phase asynchronous motor based on a direct torque control technique, which is fed through a three-phase matrix converter, is presented.

2. Matrix converter used for direct torque control

The matrix converter structure has been considered in recent years. A matrix converter is a structure that directly converts an alternating current (AC) system into another alternate system,

without the DC link interface [11, 12] and uses an array with bidirectional controllable switches to generate a controlled output voltage without frequency constraint.

The "direct" meaning is that in the matrix converter, the energy does not appear as DC, and is transmitted directly from the input to the output. But the indirect structure requires a large capacitor in the DC link, which will increase its cost. In addition, in indirect structures, if two voltage source converters are controlled, two separate control units are needed.

In simple terms, in indirect structures, two controllers are needed to control the frequency, amplitude and phase of the voltage and current signals. Also, due to the removal of the dc link, there is no need for a large reactive power storage element, and reactive power consumption is limited to small input filters [13–15]. A matrix converter provides a high degree of controllability. These converters allow independent control of the frequency, amplitude and phase of the voltage and current signals.

A special type of matrix converter with the name of the single-sided (unidirectional) matrix converter is given in reference [16]. This converter uses unidirectional switches and generates a DC pulse output that is only suitable for the drive of the brushless dc motor switched reluctance motor. In matrix converters, there must always be two rules. One is that since the matrix converter loads are usually inductive, therefore, in order to avoid interruptions of current, it is necessary at any moment, at least one of the switches connected to the output phase must be turned on. Another is that, due to the supply of these converters by the voltage source, none of the input phases do short-circuit.

In Fig. 1, according to these two rules, there are 27 allowable switching modes which produce 27 output voltage vectors based on the following equation [17, 18]:

$$\bar{v}_o = \frac{2}{3}\left(v_A + a \cdot v_B + a^2 \cdot v_C\right), \qquad a = e^{(j2\pi/3)}. \tag{1}$$

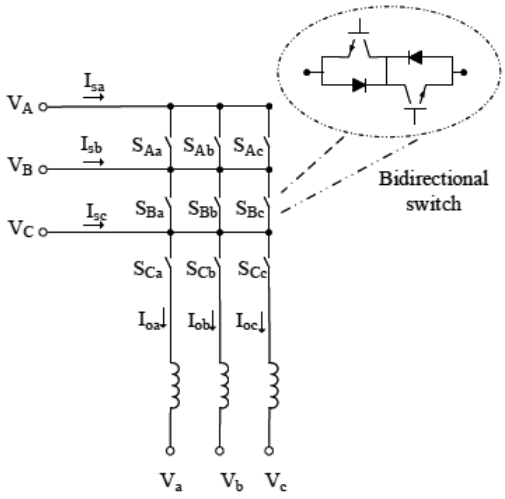

Fig. 1. 3×3 matrix converter

These 27 modes are divided into 3 groups. In the first group, output voltage vectors include six vectors with equal amplitudes and positive or negative phase sequences. In the second group

there are 18 vectors, which vary in 6 directions and have a constant phase and variable size. In the third group there are three vectors that produce zero output voltage. In this group, all three output phases are connected to a common input phase. In direct torque control with a matrix converter, only vectors of the second and third groups are used.

3. The direct predictive control of torque

Predictive control is one of the control theories introduced in the late 1970s. Given the benefits that have been raised for it, in order to improve the performance of direct torque control, the predictive control was applied to direct torque control and lead to improve torque control and current of conventional drives of direct torque control. The combined control system has better flexibility than direct torque control and the torque response is faster than the vector control method.

Given that predictive control requires more computing, and the fact that the capabilities of microprocessors have increased, in recent years, attention has been paid to this method [19, 20]. in [21], due to limitations in switch selection and torque ripple in conventional direct torque control (DTC), a control approach is presented that combines the DTC and model predictive control using direct matrix converter. But this method has a complex cost function. Fig. 2 shows the direct predictive control method of torque. According to the mentioned control algorithm, the torque reference is generated by an external speed control loop, while the reference for the size of the stator flux is kept constant. The performance of the algorithm is as follows:

- Rotor speed and stator current are measured.
- These measurements are used to predict the torque and stator flux for different switching states of the converter.
- The purpose of the estimated values according to the different switching states is to minimize the objective function F, which function is defined as a function of torque and flux.
- The voltage vector that minimizes the value of the F function is applied to the converter and thus to the terminal of the machine.

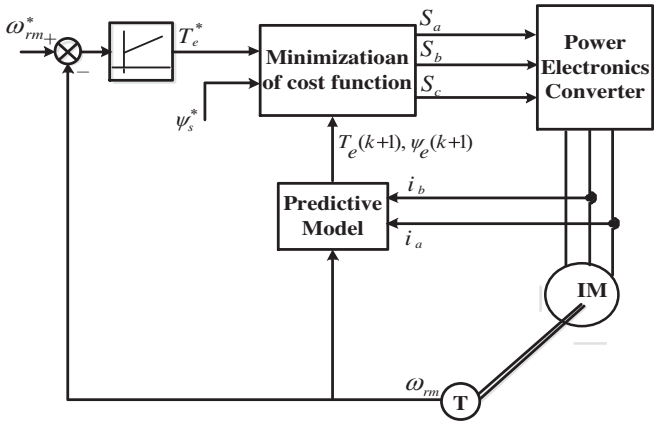

Fig. 2. Block diagram of the direct predictive control method of motor torque

4. The model of proposed method

In this section, we describe the relationships and modeling of the system under study. Fig. 3 shows the model of the proposed system, which consists of four main sections. These four sections include the induction motor model, the matrix converter model, the predictive control model, and the optimization section.

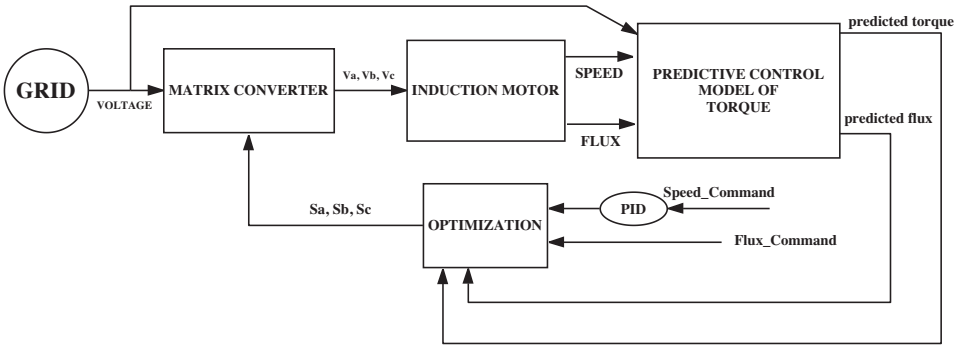

Fig. 3. The model of the proposed system

Next, the relationship between Clarke's transformation and Park's transformation is first introduced. These transformations are used to model the three phase induction motor. Thereafter, the relationship between the induction motor is given.

For modeling the induction motor, its model is used in the stationary reference frame. Then, the relationships of the predictive control are presented. The predictive control will consist of two parts. The first part presents the discrete model of the induction motor, and the second part defines the relations of the objective function.

Equation (2) shows the mathematical relation of Clarke's transformation which using it, variables go from the three-phase environment to the alpha-beta space.

$$\begin{bmatrix} x_\alpha \\ x_\beta \end{bmatrix} = \begin{bmatrix} \frac{2}{3} & \frac{-1}{3} & \frac{-1}{3} \\ 0 & \frac{1}{\sqrt{3}} & \frac{-\sqrt{3}}{3} \end{bmatrix} \begin{bmatrix} x_A \\ x_B \\ x_C \end{bmatrix}. \tag{2}$$

In the above, x_α and x_β are the space vector image in direction of α and β axes, respectively. x_A, x_B and x_C are the sinusoidal variables of phase A, B and C, respectively. Park's transformation is used to transmit space vector from the stationary frame of $\alpha-\beta$ to the rotating frame of $d-q$ at angular speed of ω. Fig. 4 shows these two environments. δ_A is the angle difference between the direction of the α axis and d axis direction. Equations (3) and (4) are also mathematical expressions of Park's transformation.

$$\delta_A = \omega t, \tag{3}$$

$$\begin{bmatrix} x_d \\ x_q \end{bmatrix} = \begin{bmatrix} \cos\delta_A & \sin\delta_A \\ -\sin\delta_A & \cos\delta_A \end{bmatrix} \begin{bmatrix} x_\alpha \\ x_\beta \end{bmatrix}. \tag{4}$$

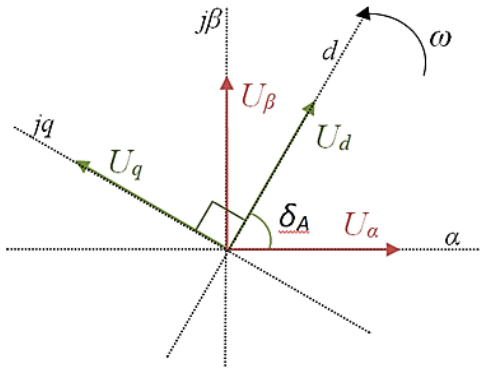

Fig. 4. Representation of α-β stationary reference frame and $d-q$ rotating reference frame

Equation (5) is used to transfer from the $d-q$ rotating reference frame to sinusoidal three-phase variables.

$$\left[T_{dqo}(\theta_r)\right]^{-1} = \begin{bmatrix} \cos\theta & \sin\theta & 1 \\ \cos(\theta-120) & \sin(\theta-120) & 1 \\ \cos(\theta+120) & \sin(\theta+120) & 1 \end{bmatrix}. \tag{5}$$

By extracting the voltage equations of the rotor and stator coils, the stator, rotor inductance matrices and stator-rotor mutual inductance matrix, the flux linkages of the stator and rotor referenced to the stator will be as follows:

$$\begin{bmatrix} \lambda_{ds} \\ \lambda_{qs} \\ \lambda_{os} \\ \lambda'_{dr} \\ \lambda'_{qr} \\ \lambda'_{or} \end{bmatrix} = \begin{bmatrix} L_{ls}+L_m & 0 & 0 & L_m & 0 & 0 \\ 0 & L_{ls}+L_m & 0 & 0 & L_m & 0 \\ 0 & 0 & L_{ls} & 0 & 0 & 0 \\ L_m & 0 & 0 & L_m+L'_{lr} & 0 & 0 \\ 0 & L_m & 0 & 0 & L_m+L'_{lr} & 0 \\ 0 & 0 & 0 & 0 & 0 & L'_{lr} \end{bmatrix} \begin{bmatrix} i_{ds} \\ i_{qs} \\ i_{os} \\ i'_{dr} \\ i'_{qr} \\ i'_{or} \end{bmatrix}. \tag{6}$$

The input power in the dqo frame using $[T_{dqo}]$ will be equal to

$$p_{in} = \frac{3}{2}\left(v_{ds}i_{ds} + v_{qs}i_{qs} + 2v_{os}i_{os} + v'_{dr}i'_{dr} + v'_{qr}i'_{qr} + 2v'_{or}i'_{or}\right). \tag{7}$$

The electromagnetic torque produced by the machine is obtained from the following:

$$T_{em} = \frac{3P}{4}\left(\lambda'_{dr}i'_{qr} - \lambda'_{qr}i'_{dr}\right) = \frac{3P}{4}\left(\lambda_{qs}i_{ds} - \lambda_{ds}i_{qs}\right) = \frac{3PL_m}{4}\left(i'_{qr}i'_{ds} - i'_{dr}i'_{qs}\right). \tag{8}$$

Also for linkage fluxes in the α-β stationary reference frame:

$$\psi_{\alpha s} = \int (v_{\alpha s} - R_s i_{\alpha s})\,\mathrm{d}t, \tag{9}$$

$$\psi_{\beta s} = \int (v_{\beta s} - R_s i_{\beta s})\,\mathrm{d}t, \tag{10}$$

$$\psi_s = \sqrt{\psi_{\alpha s}^2 + \psi_{\beta s}^2}\,. \tag{11}$$

The electromagnetic torque is simplified for the linkage fluxes as follows:

$$T_e = \frac{3P}{2}(\psi_{\alpha s} i_{\beta s} - \psi_{\beta s} i_{\alpha s}). \tag{12}$$

5. The proposed matrix converter

The switching function is defined as follows:

$$S_{ij}(t) = \begin{cases} 1 & S_{ij} \text{ closed} \\ 0 & S_{ij} \text{ open} \end{cases} \qquad i = A, B, C \;\; \therefore \;\; j = a, b, c. \tag{13}$$

The switching function has the following constraint:

$$S_{ia} + S_{ib} + S_{ic} = 1, \qquad i = A, B, C. \tag{14}$$

Generally using the switching function, there are $2^9 = 512$ switching modes.

Now, if the above constraint is applied, only 27 switching modes will be acceptable.

The constraint is based on the fact that the matrix converter should always feed the load, and no connection between the load and source can be considered. Disconnecting all the switches means that the output of that phase is interrupted which is illustrated in Fig. 5. Connecting more than one input phase to the output causes short circuit which is illustrated in Fig. 6.

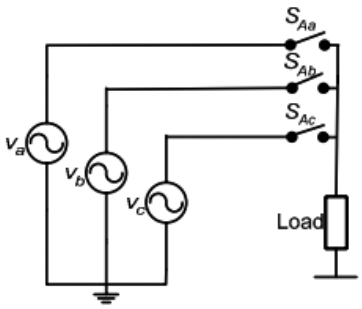

Fig. 5. Disconnection model of all phases

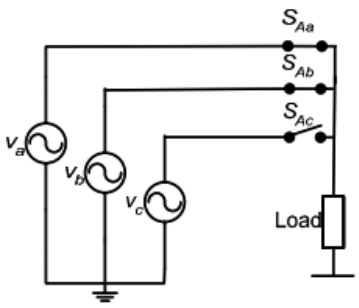

Fig. 6. Short circuit creation model

Also, in a torque predictive control model, the motor discrete time model is obtained to predict motor behavior. Considering the dynamic model of the induction motor, the predictive model of induction motor is built in $\alpha - \beta$ frame. Therefore, the relation of the electromagnetic torque is obtained as follows:

$$\begin{aligned} \overline{T}_e(k+1) &= \frac{3\rho L_m}{2(L_r L_s - L_m^2)} \mathrm{Im}\left\{\overline{\Psi}_R(k+1)\Psi_S(k+1)\right\} = \\ &= \frac{3\rho L_m}{2(L_r L_s - L_m^2)}(\Psi_{R\alpha}(k+1)\Psi_{S\beta}(k+1) - \Psi_{R\beta}(k+1)\Psi_{S\alpha}(k+1)). \end{aligned} \tag{15}$$

Therefore, the relationship between the stator and rotor flux as well as the electromagnetic torque and the predictive model of the induction motor is completed. For 27 possible switching modes, the values of the rotor and stator flux and electromagnetic torque are calculated for the next sampling moment of $k+1$. The calculated values are then sent to the optimizer and minimizer unit. The objective function is defined as follows:

$$G = \lambda_{T_e} \left| \overline{T}_e^* - \overline{T}_e^p \right| + \lambda_{\Psi_S} \left| \left\| \Psi_S^* \right\| - \left\| \Psi_S^p \right\| \right|. \tag{16}$$

In the above, λ_{T_e} is the torque weighting factor, λ_{Ψ_S} is the stator flux weight coefficient, $\overline{T}_e^*$ is the value of the electromagnetic torque reference and Ψ_S^* is the reference value of the stator flux. $\overline{T}_e^p$ is the predicted value of electromagnetic torque and Ψ_S^p is the predicted stator flux space vector. The switching vector that has the smallest value of G is selected and then applied to the matrix converter. In this way, the matrix converter operates based on the corresponding switching vector and sends the voltage to the motor terminal to generate the reference values of stator flux and electromagnetic torque.

6. Simulation

The parameters of the induction motor used in simulation are presented as follows:

The stator resistance of R_s and the rotor resistance of R_R are 1.37 and 1.1 Ω respectively. Self-inductance of stator L_S and the self-inductance of rotor L_r are 0.1459 and 0.149 H, respectively. The mutual inductance L_m is 0.141 H. The number of poles ρ is 2. The inertia of J is 0.1 kg.m^2 and the Ψ_S^* is 0.9084 Wb. The PI speed controller parameters are K_p and K_I and are determined by trial and error and are 40 and 0.01574. The sampling frequency of the system is 20 kHz.

The simulations performed on the studied system are divided into two parts. In the first section, it is assumed that the speed reference varies as a step function. Also, in the second section, speed reference variations are modeled with the ramp function. For this simulation, the speed reference is tracked by the PI controller. The PI controller receives the speed error signal and computes the torque reference.

The stator flux reference is also determined by the user as input. For a 3×3 matrix converter, we have a total of 27 switching modes, among which there are 24 active modes and 3 zero modes. In each simulation step, for 27 switching modes, 27 vectors of flux and torque are predicted and the objective function is calculated 27 times. Among these modes, the mode for which the objective function has a minimum value, is selected as the optimal mode and applied to the matrix converter.

7. Simulation results

Simulations have been done for the input reference changes of speed as a step function and the ramp function, which subsequently, the results of each scenario are presented.

7.1. Simulation results for the reference speed input as the step function

The curve of speed, torque and the stator flux size of the induction motor based on the proposed method (speed reference input as a step function) are represented in Figs. 7 to 9.

According to the speed curve in Fig. 7, it is observed that the motor follows the reference speed as well. Also, in Fig. 8, when the torque is decreased and increased, the induction motor follows well the reference load torque curve. It is also clear in Fig. 9 that the instantaneous stator flux difference with its reference value is very low, which indicates the proper performance of the control system. In Fig. 10, in all moments, the objective function has a value between 0 and 0.1. Only at the moment $t = 2.5$ s that the speed is reduced, its value has increased significantly, but has fallen very quickly again to the specified range and in other moments it has a reasonable amount. This curve indicates the proper performance of the control system in minimizing the predictive torque control objective function.

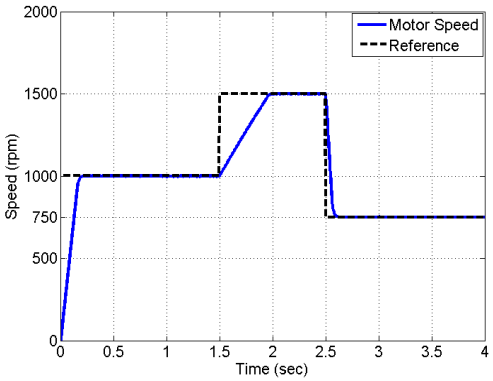

Fig. 7. The speed curve of the induction motor based on the proposed method (speed reference input as a step function)

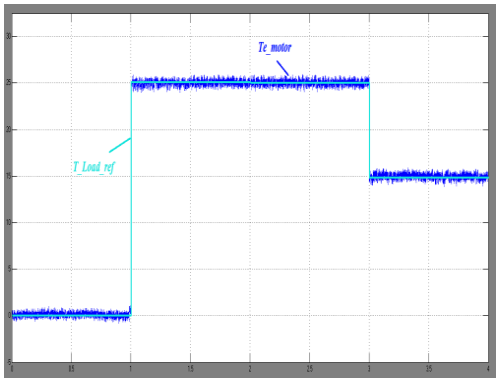

Fig. 8. The torque curve of the induction motor based on the proposed method (speed reference input as a step function)

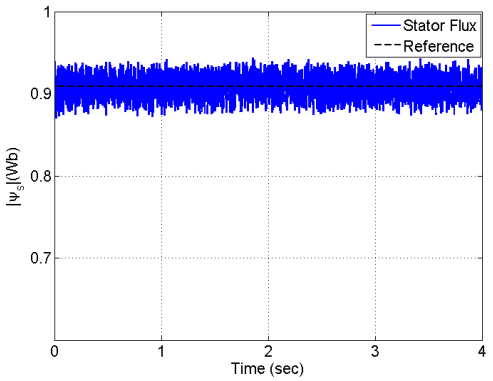

Fig. 9. The stator flux curve of the induction motor based on the proposed method (input reference speed as a step function)

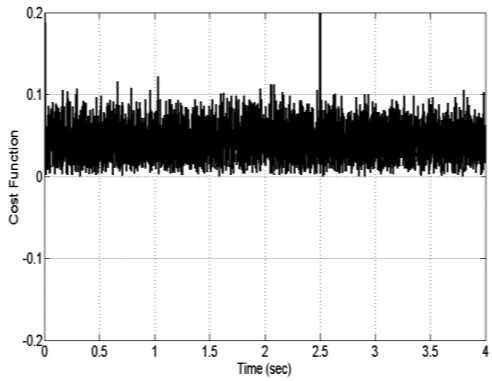

Fig. 10. Objective function curve of the direct predictive torque control method based on the proposed method (speed reference input as a step function)

Figs. 11 and 12 are respectively the response of the rotor and stator flux in the $\alpha - \beta$ environment. As it is seen the curves are circular, have low ripple and balanced shape. The current waveform of phase-A of the induction motor stator based on the proposed method (input reference speed as a step function) is illustrated by Figs. 13(a) and (b). Fig. 13(b) is the zoom of Fig. 13(a) at $t = 1$. As it seen in Fig. 13(b), at the moment of $t = 1$ s, when the torque of the motor

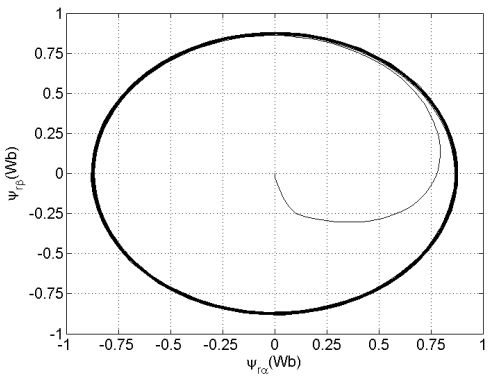

Fig. 11. The induction motor rotor flux curve based on the proposed method (input reference speed as a step function)

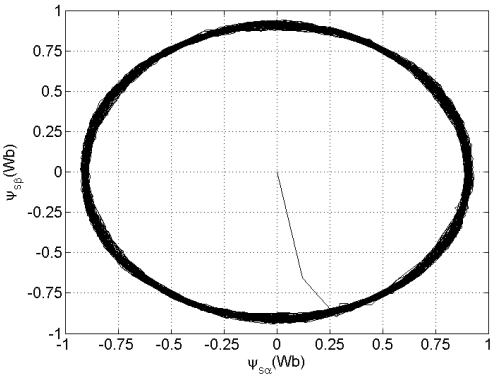

Fig. 12. The induction motor stator flux curve based on the proposed method (input reference speed as a step function)

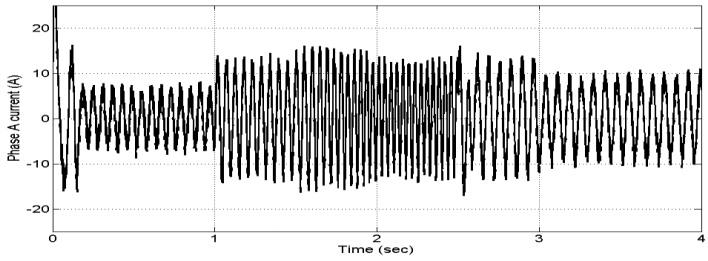

(a)

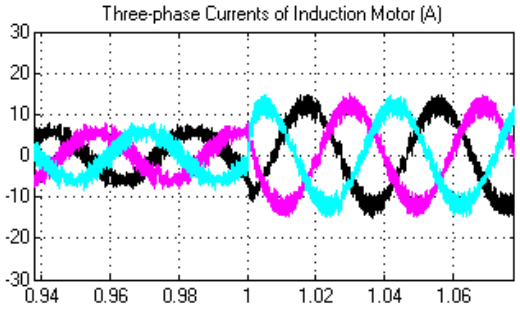

(b)

Fig. 13. The induction motor stator phase-A current curve based on the proposed method (speed reference input as step function) (a); zoom of Fig. 13(a) at $t = 1$ s (b)

load increases, the amplitude of the stator current is increased. Also, at the moment of $t = 3$ s, at which the load torque is decreased, the amplitude of the stator current is decreased.

When changing speed at moments $t = 1.5$ s and $t = 2.5$ s, to overcome the new conditions, these flow curves are subject to change.

7.2. Simulation results for speed reference input as ramp function

The curve of speed, torque and the stator flux size of the induction motor based on the proposed method (speed reference input as a ramp function) are represented in Figs. 14 to 17.

As shown in Fig. 14, the motor speed curve is fully aligned with the reference speed curve which shows the good capabilities of the control system. On the other hand, according to Fig. 15, the torque curve of the motor follows the reference torque curve changes. It is also shown in Fig. 16 that the stator instantaneous flux difference with its reference value is very low.

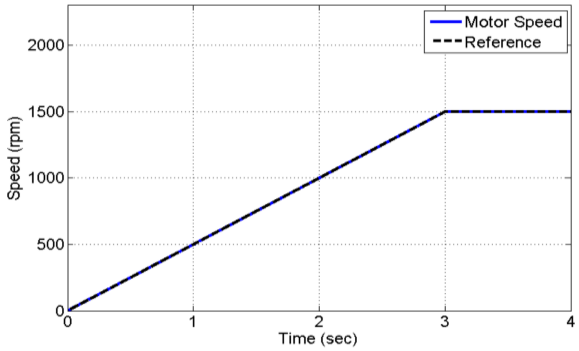

Fig. 14. The speed curve of the induction motor based on the proposed method (speed reference input as a ramp function)

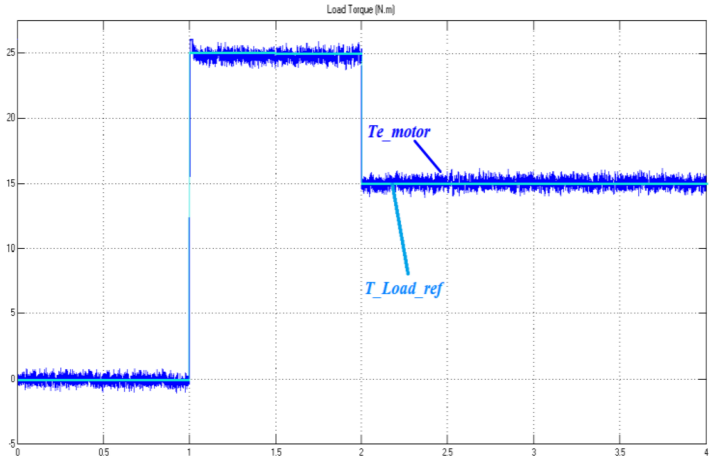

Fig. 15. The torque curve of the induction motor based on the proposed method (input reference speed as a ramp function)

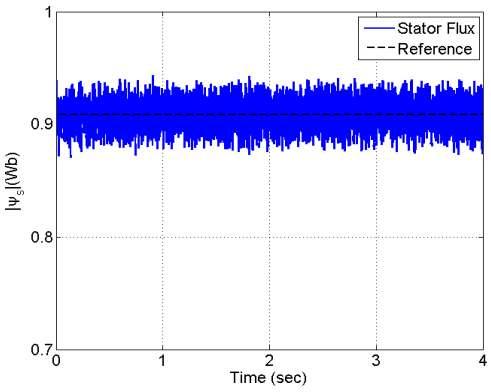

Fig. 16. The induction motor stator flux curve based on the proposed method (speed reference input as a ramp function)

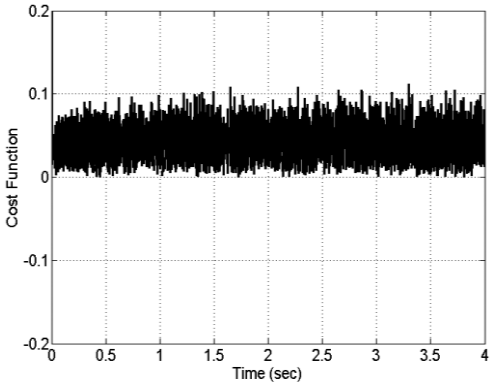

Fig. 17. Objective function curve of the direct predictive torque control method based on the proposed method (speed reference input as a ramp function)

The results also show that the stator flux curve of the induction motor follows the reference stator flux curve. The size of the objective function is shown in Fig. 17 for different moments of simulation. Given this, similar to the previous state, the minimum value of the objective function at most moments is a number between 0 and 0.1. Figs. 18 and 19 are respectively the response of the rotor and stator flux in the $\alpha-\beta$ environment. As in the previous section, the curves are circular and have a balanced shape. Of course, the flux curve of the stator has more ripple.

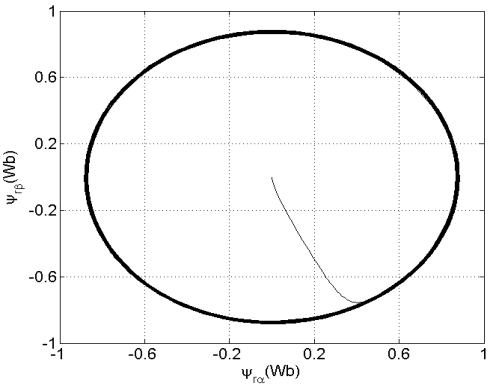

Fig. 18. The induction motor rotor flux curve based on the proposed method (input reference speed as a ramp function)

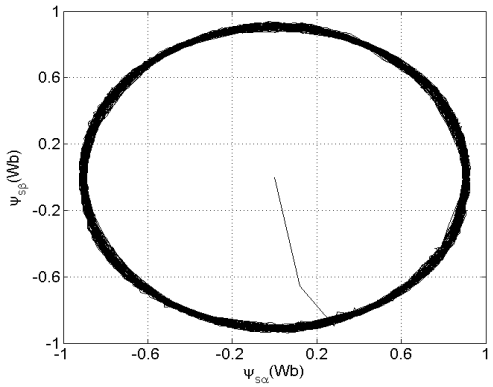

Fig. 19. The induction motor stator flux curve based on the proposed method (input reference speed as a ramp function)

The current waveform of phase-A of the induction motor stator based on the proposed method (input reference speed as a ramp function) is illustrated by Figs. 20(a) and (b). Fig. 20(b) is the zoom of Fig. 20(a) at $t = 1$ s.

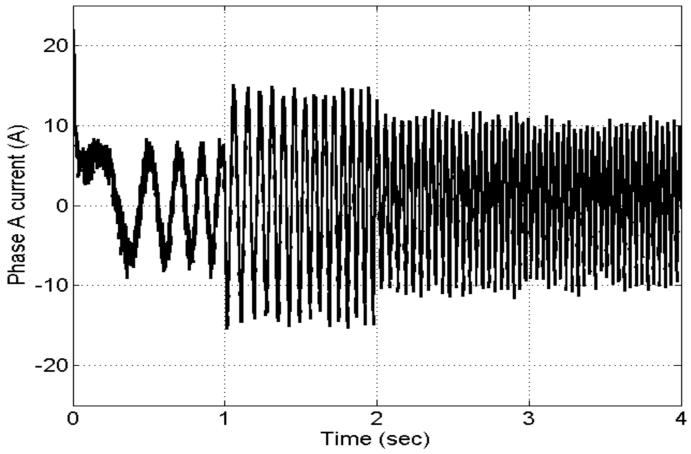

(a)

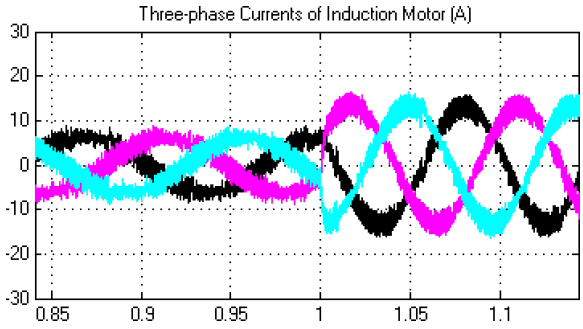

(b)

Fig. 20. The induction motor stator phase current curve based on the proposed method (speed reference input as ramp function) (a); zoom of Fig. 20(a) at $t = 1$ s (b)

As it can be seen, by increasing the load torque of the motor at the moment $t = 1$ s, the amplitude of the current drawn from the three-phase source, increases. By reducing the load torque at the moment $t = 2$ s, the stator current decreases.

7.3. Discussion about determining the weighting factors of cost function

In this section, the method of adjusting the weighting factors of the cost function is discussed. The cost function includes torque and stator flux errors. The induction motor electromagnetic torque and stator flux are the parameters which are predicted and estimated. The robustness of the system on the errors of torque and stator flux is an important point is the performance of the proposed method. According to (16), λ_{T_e} and λ_{Ψ_S} are determined by the robustness of the system as follows:

$$\lambda_{T_e} T_{\text{rated}} = \lambda_{\Psi_s} \Psi_s^* \,. \tag{17}$$

The λ_{Ψ_S} is kept constant and is equal to 1. T_{rated} is equal to 25 N.m and λ_{Ψ_S} is 0.9084 Wb. Therefore

$$\lambda_{T_e} = \frac{1 \times 0.9084}{25} = 0.036336.$$

7.4. Sensitivity analysis to induction motor parameters

In this section, the robustness and sensitivity of the proposed approach to induction motor parameters is analyzed. Robustness limits or uncertainty limits are the upper and lower limits of variation of each parameter value which the system is stable and robust. The results of each parameter are listed in Table 1.

Table 1. Robustness limits of induction motor parameters

parameter	Uncertainty limits % of change in rated value	Motor speed ω_r	Ripple of torque (N.m)	Ripple of stator flux (Wb)
$R_s = 1.37\ \Omega$	+100%	stable	0.5	0.075
	−60%	stable	1.5	0.07
$R_r = 1.1\ \Omega$	+100%	stable	1	0.07
	−90%	stable	1.5	0.075
$L_s = 0.1495$ H	+11%	stable	0.7	0.08
	−6%	stable	2	0.1
$L_r = 0.149$ H	+13%	stable	0.7	0.075
	−6%	stable	3	0.1
$L_M = 0.141$ H	+3%	stable	3.5	0.1
	−5%	stable	0.5	0.075

8. Conclusion

Given the many advantages of torque predictive control strategy as well as direct matrix converters, the integration of the variable speed drive system of the induction motor using a torque predictive control and a direct matrix converter is a novel topic.

In this paper, to achieve this aim, all of the permitted modes for matrix converter switching are presented first. Then, flux and torque prediction operations were performed for all allowed switching states. By optimizing the cost function based on the error of the flux and the reference torque relative to the predicted flux and torque, in each simulation step, the best switching mode is extracted and applied to the matrix converter.

For validation of the method presented in this paper, numerical simulation is provided using the Matlab/simulink software. The induction motor drive system has been tested for different reference values of torque and speed, the results of which indicate the proper functioning of the control system. The simulations have been done for speed reference input as a step and ramp function.

The results show that using the proposed control method, the motor speed curve completely coincides with the reference speed curve, the torque curve of the motor follows the reference torque curve variations, the instantaneous stator flux difference is very low with its reference value. The stator flux curve of the induction motor follows the reference stator flux curve.

References

[1] Cortes P., Kazmierkowski M.P., Kennel R.M., Quevedo D.E., and Rodriguez J., *Predictive control in power electronics and drives*, IEEE Trans. Ind. Electron., vol. 55, no. 12, pp. 4312–4324 (2008).

[2] Miranda H., Cortes P., Yuz J., Rodriguez J., *Predictive torque control of induction machines based on state-space models*, IEEE Trans. Ind. Electron., vol. 56, no. 6, pp. 1916–1924 (2009).

[3] Riveros J.A., Barrero F., Levi E., Duran M.J., Toral S., Jones M., *Variable-speed five-phase induction motor drive based on predictive torque control*, IEEE Trans. Ind. Electron., vol. 60, no. 8, pp. 2957–2968 (2013).

[4] Klumpner C., Nielsen P., Boldea I., Blaabjerg F., *A new matrix converter motor (MCM) for industry applications*, IEEE Trans. Ind. Electron., vol. 49, no. 2, pp. 325–335 (2002).

[5] Curkovic M., Jezernik K., Horvat R., *FPGA-based predictive sliding mode controller of a three-phase inverter*, IEEE Trans. Ind. Electron., vol. 60, no. 2, pp. 637–644 (2013).

[6] Davari S.A., Khaburi D.A., Wang F., Kennel R.M., *Using full order and reduced order observers for robust sensorless predictive torque control of induction motors*, IEEE Trans. Power Electron., vol. 27, no. 7, pp. 3424–3433 (2012).

[7] Karamanakos P., Stolze P., Kennel R.M., Manias S., Mouton H.D.T., *Variable switching point predictive torque control of induction machines*, IEEE Journal of Emerging and Selected Topics in Power Electron., vol. 2, no. 2, pp. 285–295 (2014).

[8] Marei M.I., *A unified control strategy based on phase angle estimation for matrix converter interface system*, IEEE Systems Journal, vol. 6, no. 2, pp. 278–286 (2012).

[9] Nikkhajoei H., Tabesh A., Iravani R., *Dynamic model of a matrix converter for controller design and system studies*, IEEE Trans. Power Del., vol. 21, no. 2, pp. 744–754 (2006).

[10] Espina J., Ortega C., Lillo L.D., Empringham L., Balcells J., Arias A., *Reduction of output common mode voltage using a novel SVM implementation in matrix converters for improved motor lifetime*, IEEE Trans. Ind. Electron., vol. 61, no. 11, pp. 5903–5911 (2014).

[11] Lee M.Y., Wheeler P., Klumpner C., *Space-vector modulated multilevel matrix converter*, IEEE Trans. Ind. Electron., vol. 57, no. 10, pp. 3385–3394 (2010).

[12] Hojabri H., Mokhtari H., Liuchen C., *A generalized technique of modeling, analysis, and control of a matrix converter using SVD*, IEEE Trans. Ind. Electron., vol. 58, no. 3, pp. 949–959 (2011).

[13] Wheeler P., Grant D.A., *Optimized input filter design and low-loss switching techniques for a practical matrix converter*, Proc. Inst. Elect.Eng. Elect. Power Appl., vol. 144, no. 1, pp. 53–60 (1997).

[14] Helle L., Larsen K.B., Jorgensen A.H., Munk-Nielsen S., Blaabjerg F., *Evaluation of modulation schemes for three-phase to three-phase matrix converters*, IEEE Trans. Ind. Electron., vol. 51, no. 1, pp. 158–171 (2004).

[15] Kolar J.W., Friedli T., Rodriguez J., Wheeler P.W., *Reviewof three-phase PWM ac-ac converter topologies*, IEEE Trans. Ind.Electron. – Special Section Matrix Converters, vol. 58, no. 11, pp. 4988–5006 (2011).

[16] Huang X., Bradley K., Goodman A., Gerada C., Wheeler P., Clare J., Whitley C., *Fault- tolerance analysis of multi-phase single sided matrix converter for brushless DC drives*, in Proc. IEEE ISIE, pp. 3168–3173, June 4–7 (2007).

[17] Yan Z., Jia M., Zhang C., Wu W., *An integration SPWM strategy for High-Frequency link matrix converter with adaptive commutation in one step based on de-re-coupling idea*, IEEE Trans. Ind. Electron., vol. 50, no. 1, pp. 116–128 (2012).

[18] Babaei E., *A cascade multilevel converter topology with reduced number of switches*, IEEE Trans. Ind. Electron., vol. 23, no. 6, pp. 2657–2664 (2008).

[19] Zhang Y., Yang H., *Model predictive torque control of induction motor drives with optimal duty cycle control*, IEEE Trans. Power. Electron., vol. 29, no. 12, pp. 6593–6603 (2014).

[20] Cho Y., Bak Y., Lee K.B., *Torque-Ripple Reduction and Fast Torque Response Strategy for Predictive Torque Control of Induction Motors*, IEEE Transactions on Power Electronics, vol. 33, no. 3, pp. 2458–2470 (2017).

[21] Peng T., Wen M., Li Z., Xu Z., Yang, J., *An improved DTC strategy for induction motors fed by direct matrix converter*, IEEE, Chinese Automation Congress (CAC), pp. 1766–1771 (2015). IEEE Transactions on Magnetics, vol. 54, iss. 6 (2018).